

PAPER • OPEN ACCESS

## A numerical solution for the axisymmetric flow of a plastic tube on a rigid fibre

To cite this article: Thanh Nguyen *et al* 2017 *J. Phys.: Conf. Ser.* **885** 012018

View the [article online](#) for updates and enhancements.

You may also like

- [Thickness dependence of fracture behaviour in a superconducting strip](#)  
H D Yong, C Xue and Y H Zhou
- [Failure load and stress intensity factor of single-lap steel joints bonded with nano- \$\text{Al}\_2\text{O}\_3\$  reinforced epoxy adhesive](#)  
Sunil Kumar Gupta
- [Numerical analysis of the mechanical and electrical properties of \(RE\)BCO tapes with multiple edge cracks](#)  
Jintao Ma and Yuanwen Gao



**ECS**  
The  
Electrochemical  
Society  
Advancing solid state &  
electrochemical science & technology

**DISCOVER**  
how sustainability  
intersects with  
electrochemistry & solid  
state science research

# A numerical solution for the axisymmetric flow of a plastic tube on a rigid fibre

Thanh Nguyen<sup>1</sup>, Kien Nguyen<sup>2</sup>, Sergei Alexandrov<sup>3</sup>

<sup>1</sup> Institute of Mechanics – VAST, Ha Noi, Viet Nam

E-mail: manhthanh2012209@gmail.com

<sup>2</sup> University of Communications and Transport, Ha Noi, Viet Nam

E-mail: ntkien@utc.edu.vn

<sup>3</sup> Institute for Problems in Mechanics - Russian Academy of Sciences

Moscow, Russia. E-mail: sergei\_alexandrov@yahoo.com

manhthanh2012209@gmail.com

**Abstract.** In the case of rigid perfectly plastic material the strain rate intensity factor appears in the vicinity of maximum friction surfaces. This factor controls the magnitude of the equivalent strain rate in a narrow region near the surface. On the other hand, the equivalent strain rate controls the evolution of material surfaces. Therefore, the existence of the strain rate intensity factor in theoretical solutions are in qualitative agreement with experimental observations that demonstrate that a narrow layer with drastically modified microstructure is often generated in the vicinity of frictional interfaces in machining and deformation processes. In order to use the strain rate intensity factor for describing such material behaviour, it is necessary to develop an efficient numerical method for calculating the strain rate intensity factor. Since this factor is involved in a singular series expansion, it is evident that commercial finite element packages are not capable of calculating the strain rate intensity factor. In the case of Tresca's solids the theory of characteristics can be used for the development of the method in question. This paper presents a first step in this direction

**Keywords:** strain rate intensity factor, rigid perfectly plastic material, axisymmetric flow, total plasticity

## 1. Introduction

Numerous experimental observations demonstrate that a narrow layer with drastically modified microstructure is generated near frictional interfaces in machining and deformation processes. This layer is usually called white layer in papers devoted to machining processes and fine grain layer in papers devoted to metal forming processes. A complete review of results on white layer/fine grain layer generation published before 1987 has been presented in [1]. According to this review article there are three main contributory mechanisms responsible for white layer generation. One of these mechanisms is the mechanism of intensive plastic deformation. This mechanism can be described by means of the strain rate intensity factor introduced in [2]. This factor is the coefficient of the leading singular term in a series expansion of the equivalent strain rate near maximum friction surfaces. This expansion shows that the equivalent strain rate is infinite at the friction surface. Therefore, the strain



rate intensity factor controls the magnitude of the equivalent strain rate in its vicinity. On the other hand, the equivalent strain rate controls the evolution of material properties. In the case of rigid perfectly plastic materials a necessary condition for the existence of the strain rate intensity factor is the friction boundary condition that postulates that the friction stress at sliding is equal to the shear yield stress (maximum friction law). This boundary condition is often adopted at the tool - chip interface (at least, over a portion of this interface) in machining processes [3 - 10]. This zone is usually called the sticking zone. The existence of such zones has been reported in deformation processes as well [11 - 14]. However, it is worthy of note that the actual seizure (the velocity vector is continuous across the interface) may or may not occur in theoretical solutions. It depends on the constitutive equations chosen. Also, the interpretation of experimental results on this issue is controversial [15]. In the present paper, it is assumed that sliding occurs at maximum friction surfaces. In this case models for describing the generation of fine grain layers near frictional interfaces based on the strain rate intensity factor have been proposed in [16, 17]. In order to apply these models to industrial problems, it is necessary to carry out a special experimental program and to develop an accurate method for calculating the strain rate intensity factor. Since this factor is involved in a singular asymptotic expansion of the equivalent strain rate, it is evident that commercial finite elements packages are not capable of calculating the strain rate intensity factor. Probably, the generalized finite element method [18] can be used for this purpose. However, no specific code is currently available. To the best of authors' knowledge, the only available numerical approach for calculating the strain rate intensity factor is based on the method of characteristics [19]. This approach is valid for plane strain deformation of rigid perfectly plastic material. On the other hand, most of experimental results are available for axisymmetric deformation, for example [20, 21]. Using analytic and semi-analytic solutions the strain rate intensity factor in axisymmetric flows has been determined in [22, 23]. However, comparison of the accurate numerical plane strain solution derived in [19] and the corresponding approximate analytic solution demonstrates that the accuracy of the analytic solution is not sufficient for practical applications. Therefore, an efficient numerical method for calculating the strain rate intensity factor in axisymmetric flow is needed. In the case of Tresca's solids (i.e. solids satisfying Tresca's yield criterion and its associated flow rule) such a method can be based on the theory of characteristics and can be considered as an extension of the method developed in [19]. In particular, the general theory of characteristics for this case is presented in [24]. In the present paper, as a first step to the development of a numerical method for calculating the strain rate intensity factor in axisymmetric flows, this theory is used in the conjunction with the finite difference method to build up the field of characteristics and, as a result, the field of stress for the problem formulated in [23] but without using simplified assumptions accepted in this paper. Then, comparison of the numerical and analytic solutions is made.

## 2. Boundary value problem and constitutive equations

Consider the compression of rigid perfectly plastic tube on a rigid fibre of radius  $a$  (Fig. 1). The outer radius of the tube is  $b$  and its inner radius is  $a$ . The length of both the fibre and tube is  $2L$ . Pressure applied at the outer surface of the tube causes axisymmetric plastic deformation in it. Cylindrical coordinate system  $(r, \theta, z)$  is taken such that the  $z$ -axis coincides with the axis of symmetry of the flow and the plane  $z = 0$  is the plane of symmetry. Then, it is sufficient to consider the region  $0 \leq z \leq L$ . The non-zero stress components are denoted by  $\sigma_r$ ,  $\sigma_\theta$ ,  $\sigma_z$ , and  $\tau_{rz}$ . Velocity components in the radial and axial directions are denoted by  $v_r$  and  $v_z$  respectively. The boundary conditions are

$$\tau_{rz} = 0 \quad \text{at} \quad r = b, \quad (1a)$$

$$\tau_{rz} = k \quad \text{at} \quad r = a, \quad (1b)$$

$$\sigma_z = 0 \quad \text{and} \quad \tau_{rz} = 0 \quad \text{at} \quad z = L \quad (1c)$$

$$v_r = -U \quad \text{at} \quad r = b, \quad (2a)$$

$$v_r = 0 \quad \text{at} \quad r = a. \quad (2b)$$

here  $k$  is shear yield stress. On the plane  $z = 0$ , by symmetry

$$v_z = 0 \quad \text{and} \quad \tau_{rz} = 0 \quad (3)$$

In the present problem, the case of interest is that in which  $v_r \leq 0$ . Then, under conditions of axial symmetry, it is assumed that the material of the tube satisfies Tresca's yield criterion in the regime of total plasticity (see, for example [24, 25]), so that

$$(\sigma_r - \sigma_z)^2 + 4\tau_{rz}^2 = 4k^2 \quad ; \quad \sigma_\theta = \frac{1}{2}(\sigma_r + \sigma_z) - k \quad (4)$$

The stress components satisfy the equilibrium equations

$$\frac{\partial \sigma_r}{\partial r} + \frac{\partial \tau_{rz}}{\partial z} + \frac{\sigma_r - \sigma_\theta}{r} = 0 \quad (5a)$$

$$\frac{\partial \tau_{rz}}{\partial r} + \frac{\partial \sigma_z}{\partial z} + \frac{\tau_{rz}}{r} = 0 \quad (5b)$$

and, there are four equations for the determination of the four unknown stress components, i.e. the problem is statically determinate.

The velocity components are determined by the incompressibility and isotropy conditions

$$\frac{\partial v_r}{\partial r} + \frac{v_r}{r} + \frac{\partial v_z}{\partial z} = 0 \quad (6)$$

$$\left(\frac{\partial v_r}{\partial z} + \frac{\partial v_z}{\partial r}\right) / \left(\frac{\partial v_r}{\partial r} - \frac{\partial v_z}{\partial z}\right) = 2\tau_{rz} / (\sigma_r - \sigma_z) \quad (7)$$

It is known that these systems (i.e. (5a)-(5b) and (6)-(7)) are hyperbolic and the characteristics for the stresses and the velocities coincide, furthermore, they coincide with the slip-lines. Therefore, there are two distinct characteristic directions at a point, denoted by  $\alpha$  and  $\beta$  respectively. In such a case the method of characteristics can be used to solve the problem under consideration. Substituting

$$\sigma_r, \sigma_z = \sigma \pm k \sin 2\varphi, \quad \tau_{rz} = k \cos 2\varphi \quad (8)$$

here  $\sigma = (\sigma_r + \sigma_z)/2$  and  $\varphi$  is the anti-clockwise angular rotation of the  $\alpha$ -line from the  $z$ -axis. Then, equations for  $\alpha$ -lines and  $\beta$ -lines are

$$dr/dz = \tan \varphi \quad \text{and} \quad dr/dz = -\cot \varphi \quad (9)$$

Now the  $\alpha$ -line and  $\beta$ -line are regarded as a pair of right-handed curvilinear axes of reference and denoted by  $s_\alpha$  and

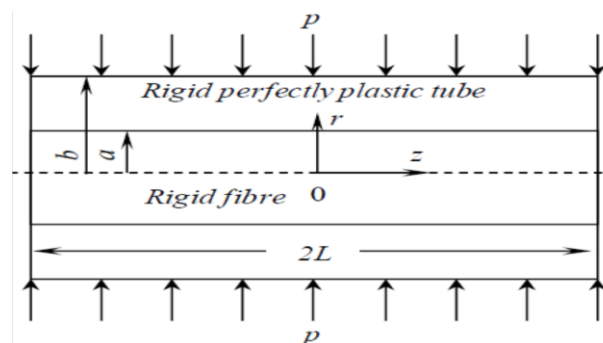


**Figure 1.** Configuration and coordinate system.

$s_\beta$  respectively. Then, following [24] in transforming from the coordinate system  $(z, r)$  to the characteristic coordinates  $(s_\alpha, s_\beta)$ , with  $v_\alpha$  and  $v_\beta$  being the components of the velocity vector along the characteristic coordinates, the equations (5a), (5b), (6) and (7) take the form

$$d\sigma - 2kd\varphi = \frac{k}{r}(-dr - dz) \quad \text{along an } \alpha\text{-line} \quad (10a)$$

$$d\sigma + 2kd\varphi = \frac{k}{r}(-dr + dz) \quad \text{along a } \beta\text{-line} \quad (10b)$$

$$dv_\alpha - v_\beta d\varphi = -\frac{1}{2r}(v_\alpha dz - v_\beta dr) \text{ along an } \alpha\text{-line} \quad (11a)$$

$$dv_\beta + v_\alpha d\varphi = -\frac{1}{2r}(v_\alpha dr + v_\beta dz) \text{ along a } \beta\text{-line} \quad (11b)$$

and the boundary conditions (1a-b-c) and (2a-b) become

$$\varphi = 7\pi/4 \text{ at } r = b, \quad (12a)$$

$$\varphi = 2\pi \text{ at } r = a, \quad (12b)$$

$$\sigma = -k \text{ and } \varphi = 7\pi/4 \text{ at } z = L \quad (12c)$$

$$v_\beta = v_\alpha - U\sqrt{2} \text{ at } r = b, \quad (13a)$$

$$v_\beta = 0 \text{ at } r = a. \quad (13b)$$

### 3. Numerical solution

#### 3.1. Numerical scheme for the problem of Sect. 2

Small displayed equations: Some examples: Several numerical schemes based on the method of characteristics have been proposed to determine the stress and velocity distributions in axisymmetric flow of rigid perfectly plastic solids [24]. In the present paper we adopt one of these scheme, which is analogue to the scheme presented in [19, 26] for the problem in plane strain flow, to solve the problem formulated in the previous section.

The general structure of the characteristics and Cartesian coordinates ( $z, r$ ) are symbolically illustrated in Fig. 2. Starting from base-line AB, the stress distribution across a network of characteristics (slip-lines) can be uniquely defined by using the systems (9), (10a-b), and the boundary conditions (12a-b-c). The equations (9), (10a-b) (expressed in finite-difference form) are nonlinear and solved by suitable iterative procedures.

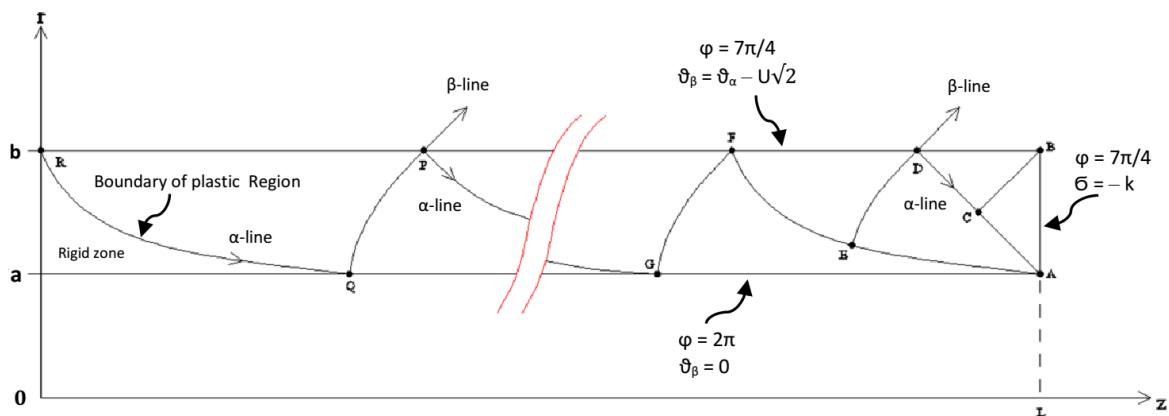


**Figure 2.** Configuration and coordinate system ( $z \geq 0, r \geq 0$ ).

The stress solution and slip-line field in the region ABC are determined by the conditions (12c) at  $N$  equally spaced nodal points on the segment AB. The nodal points on  $\beta$ -line BC were taken as the intersections with the  $\alpha$ -lines (through the nodal points on AB). The nodal points on  $\alpha$ -line AC were taken in a similar way. Next, the field BCD is defined by the solutions on BC and the boundary condition (12a). The point A is a singularity through which pass all  $\alpha$ -lines within an angle of  $45^\circ$  between AD and AG. Having the solutions on AD, the field ADE is defined by the numerical procedure proposed in [24, 27]. The construction of the field continues in similar way up to the slip-line through the point R located on the intersection of the plane  $z = 0$  with the outer surface of the tube. This curve is the  $\alpha$ -line and also the boundary between the rigid and plastic regions.

Having completed the slip-line field, the velocity solution is built up from the left in Fig. 2 and uniquely determined by the conditions for the velocities on BR, AQ and RQ. At this moment a suitable velocity boundary conditions should be set on the rigid plastic boundary RQ. The wedge shaped area included between RQ and its counterpart in the left-hand quadrant is rigid and do not move down as a whole body but lose material to the plastic region. Using (11a), (12a) and taking into account that the normal component of velocity vector is continuous across RQ yield

$$v_{\beta} = 0 \quad , \quad v_{\alpha} = U \cdot \sqrt{2b/r} \quad \text{on RQ} \quad (14)$$

It is evident that the tangential component of velocity  $v_{\alpha}$  is discontinuous across RQ.

Now that all the velocity boundary conditions have been identified, starting from rigid plastic boundary RQ, the velocity solution can be found using linear system of equations (11a-b) in finite-difference form. The construction of the velocity field is almost identical to the one used in the stress determination.

### 3.2. Numerical results and comparisons.

An analytic solution to the problem formulated in the section 2 has been given by Spencer A. J. M. in [25]. This solution is approximate because the boundary conditions at  $z = 0$  and  $z = L$  are ignored. However, all the equations and the boundary conditions at  $r = a$  and  $r = b$  are satisfied. Since Spencer's solution gives a good approximation to the solution for compression of rigid perfectly plastic tube on a rigid fibre, except near the ends and center of the tube, it is inferred that Spencer's solution is appropriate to verify numerical results obtained here if the length of the tube is large enough compared to its radius. Note that when calculating the stress and velocity fields by Spencer's formula, the following boundary conditions in the integral form have been used [23]

$$\int_a^b r \sigma_z|_{z=L} dr = 0, \quad \int_a^b r v_z|_{z=0} dr = 0 \quad (15)$$

Without loss of generality, it is assumed that  $U = 1$  and  $(b - a) = 1$ . The calculations were performed for tubes with a ratio  $L / (b - a)$  in the range of 5 – 25, and an inner radius  $a$  in the range of 1–20. Fig. 3 shows two slip-line field configurations corresponding to  $\{L = 5.54, a = 1\}$  and  $\{L = 6.25, a = 3\}$  respectively. In both cases, the number of nodes  $N$  on the segment AB are equal to 6. It is seen from Fig. 3 that both families of characteristics are straight in the triangle ABD in which the two relationships are satisfied :  $dr = -dz$  along an  $\alpha$ -line and  $dr = dz$  along a  $\beta$ -line, therefore all the stress components are constant by (8) and (10a-b). Thus, the stress state is uniform in the region ABD.

Next, the radial stress and axial velocity distributions on AQ (along the friction surface  $r = a$ ) for the both numerical and analytic solutions are compared in Fig. 4. With  $N = 11$ , the calculations were performed for the tube with  $L = 13.86, a = 1$ . In this case, as expected, the numerical and analytic solutions for  $\sigma_r$  and  $v_z$  are very closed to each other when the variable  $z$  lies in the distances greater than  $2(b - a)$  from the ends and greater than  $3(b - a)$  from the center of the tube.

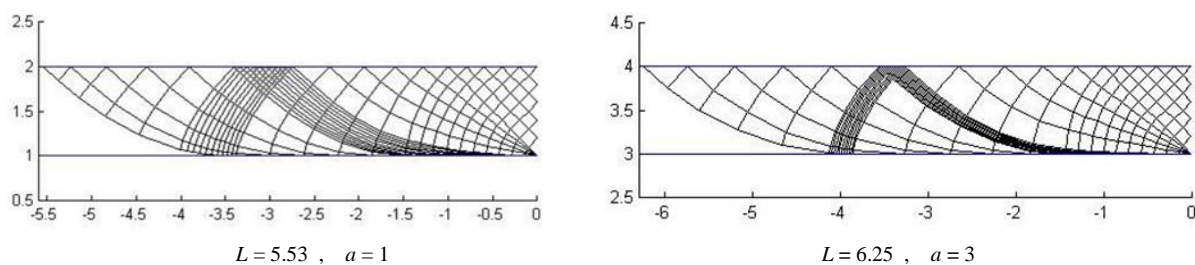


**Figure 3.** Slip-line fields calculated for tubes of different radius and length-diameter ratio ( $N = 6$ ).

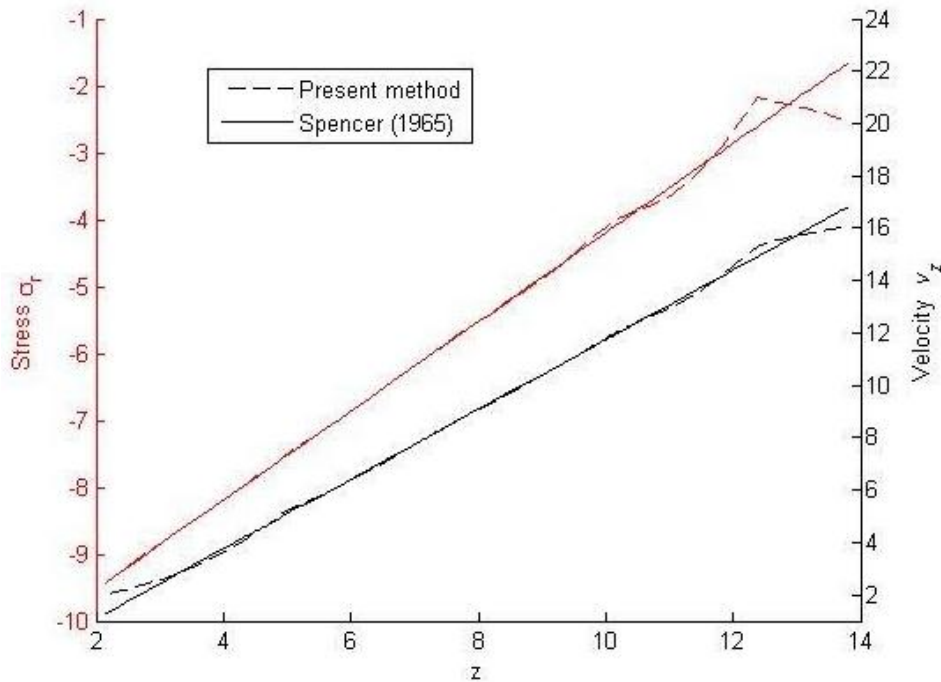


**Figure 4.** Comparison of numerical and analytical values of  $\sigma_r, v_z$  along the friction surface  $r = a$  ( $L = 13.86, N = 11$ ).

Considering that Spencer’s solution is accurate, at least in places situated at a long enough distance from the center and the ends of the tube, it is reasonable to introduce the following definitions for the investigation of the distribution of relative error within the plastic region:

$\beta$  - a set of all the nodal points on the  $\beta$ -line, which is selected for comparison.

$\beta_L|z_a$  - a set of all the nodal points on the  $\beta$ -line passing through point  $(z = z_a, r = a)$ .

$\delta(f|\beta)$  - the maximum absolute value of the relative error of the value  $f$  in the set  $\beta$

$$\delta(f|\beta) = \max_{(z_i, r_i) \in \beta} \left| \frac{f^{(A)}(z_i, r_i) - f^{(N)}(z_i, r_i)}{f^{(A)}(z_i, r_i)} \right| \tag{16}$$

here  $f^{(A)}(z_i, r_i)$  and  $f^{(N)}(z_i, r_i)$  are the calculated values of Spencer’s and numerical solutions respectively at  $(z_i, r_i)$ .

Now there are three  $\beta$ -lines selected within the plastic region for each tube. The first passing through point  $(z_a, a)$  located close to the end of the tube, but  $z_a < L - 2(b - a)$ . The second passing through the point located near the middle of AQ. The third passing through point  $(z_a, a)$  located close to the center of the tube, but  $z_a > z_Q$  (the  $z$ -coordinate of the point Q). The positions of these  $\beta$ -lines are relatively specific to the distribution of the calculated values. Having calculated the stress and velocity fields (for two cases  $L = L1 = 13.86, L = L2 = 22.2$  with  $N = 11$ ) according to Spencer’s and numerical solutions, the maximum relative errors of all the calculated values on the above selected  $\beta$ -lines are found from (16) and presented in Tab. I. It is seen from this table that the relative errors are very small for the middle  $\beta$ -lines despite the number  $N$  is relatively small. Also, the error decreases as the length-diameter ratio increase over plastic zone except the ends.

**Table 1.** Relative Errors of Numerical values.

Set $\beta$	Maximum Value of The Relative Error				
	$\delta(\tau_{rz} \beta)$	$\delta(\sigma_r \beta)$	$\delta(\sigma_z \beta)$	$\delta(v_r \beta)$	$\delta(v_z \beta)$
$\beta_{L1} _{11.82}$	3.9e-1	2.9e-3	5.6e-2	2.2e-1	5.2e-3
$\beta_{L2} _{20.2}$	7.0e-2	3.4e-2	1.3e-1	2.7e-1	5.0e-3
$\beta_{L1} _{7.7}$	2.7e-2	2.1e-3	1.4e-3	1.0e-2	1.9e-4
$\beta_{L2} _{11.21}$	1.9e-4	6.5e-4	8.4e-4	7.5e-4	4.2e-3
$\beta_{L1} _{2.83}$	3.6e-4	5.9e-4	7.8e-4	3.0e-1	2.5e-2
$\beta_{L2} _{3.07}$	5.5e-4	5.6e-4	6.4e-4	8.4e-2	0.9e-5

#### 4. Conclusion

A numerical approach for determining the stress and velocity fields of rigid perfectly plastic material in axisymmetric flows of a plastic tube on a rigid fibre has been performed. The approach is based on the method of characteristics. The accuracy of the numerical results has been verified by comparison with an accurate analytic solution. If the length-diameter ratio of the tube is large enough, the magnitude of the stress and velocity components at the places situated in the distances by 2-3 times the tube thickness from its ends and center is very close to that found from the approximate solution in which the end effects are neglected.

Since the determination of the strain rate intensity factor is based on the derivation of the equivalent strain rate in the vicinity of an envelope of characteristics, the calculation of the velocity and characteristic field with high accuracy is of high importance, therefore the numerical approach presented in the present paper is the first and right step to the development of a numerical method for calculating the strain rate intensity factor in axisymmetric flows.

#### Acknowledgments

The research described has been supported by the grants VAST.HTQT.Nga.02/16-17 (Vietnam) and RFRB-16-51-540001 (Russia).

#### References

- [1] Griffiths B.J. (1987) Mechanisms of White Layer Generation with Reference to Machining and Deformation Processes, Trans. ASME J. Tribol, 109, 525-530.
- [2] Alexandrov S., Richmond O. (2001) Singular Plastic Flow Fields near Surfaces of Maximum Friction Stress, Int. J. Non-Linear Mech. 36, 1-11.
- [3] Ng E.-G., Aspinwall D.K., Brazil D., Monaghan J. (1999) Modelling of Temperature and Forces When Orthogonally Machining Hardened Steel, Int. J. Mach. Tool Manu., 39, 885-903.
- [4] Yiğit K., Tuğrul Ö. (2006) Predictive Analytical and Thermal Modeling of Orthogonal Cutting Process—Part I: Predictions of Tool Forces, Stresses, and Temperature Distributions, J. Manu. Sci. Eng., 128, 435-444.
- [5] Ramesh A., Melkote Shreyes N. (2008) Modeling of White Layer Formation under Thermally Dominate Condition in Orthogonal Machining of Hardened AISI 52100 Steel, Int. J. Mach. Tool. Manu., 48, 402-414.
- [6] Lalwani D.I., Mehta N.K., Jain P.K. (2009) Extension of Oxley's Predictive Machining Theory for Johnson and Cook Flow Stress Model, J. Mater. Process. Tech., 209, 5305-5312.
- [7] Akbar F., Mativenga Paul T., Sheikh M.A. (2010) An Experimental and Coupled Thermo-Mechanical Finite Element Study of Heat Partition Effects in Machining, Int. J. Adv. Manuf. Technol. 46, 491-507.
- [8] Molinari A., Cheriguene R., Miguelez H. (2012) Contact Variables and Thermal Effects at the

- Tool-chip Interface in Orthogonal Cutting, *Int. J. Solids. Struct.*, 49, 3774-3796.
- [9] Chen G., Li J., He Y., Ren C. (2014) A New Approach to The Determination of Plastic Flow Stress and Failure Initiation Strain for Aluminium Alloys Cutting Process, *Comp. Mater. Sci.*, 95, 568-578.
- [10] Agmell M., Ahadi A., Stahl J.-E. (2014) Identification of Plastic Constants from Orthogonal Cutting and Inverse Analysis, *Mech. Mater.*, 77, 43-51.
- [11] Kim T.-K., Ikeda K. (2000) Flow Behavior of the Billet Surface Layer in Porthole Die Extrusion of Aluminium, *Metall. Mater. Trans.*, 31A, 1635-1643.
- [12] Widerøe F., Welo T. (2012) Conditions for Sticking Friction between Aluminium alloy AA6060 and Tool Steel in Hot Forming, *Key Eng. Mat.*, 491, 121-128.
- [13] Sanabria V., Mueller S., Gall S., Reimers W. (2014) Investigation of Friction Boundary Conditions During Extrusion of Aluminium and Magnesium Alloys, *Key Eng. Mat.*, 611-612, 997-1004.
- [14] Sanabria V., Mueller S., Reimers W. (2014) Microstructure Evolution of Friction Boundary Layer During Extrusion of AA 6060, *Proc. Eng.*, 81, 586-591.
- [15] Jaspers S.P.F.C., Dautzenberg J.H. (2002) Material Behaviour in Metal Cutting: Strains, Strain Rates and Temperature in Chip of Formation, *J. Mater. Process. Tech.*, 121, 123-135.
- [16] Goldstein R.V., Alexandrov S.E. (2015) An Approach to Prediction of Microstructure Formation Near Friction Surfaces at Large Plastic Strains, *Phys. Mesomech.*, 18, 223-227.
- [17] Alexandrov S.E., Goldstein R.V. (2015) On Constructing Constitutive Equations in Metal Thin Layer near Friction Surfaces in Material Forming Processes, *Dokl. Phys.*, 60, 39-41.
- [18] Fries T.-P., Belytschko T. (2010) The Extended/Generalized Finite Element Method: An Overview of the Method and Its Applications, *Int. J. Numer. Meth. Eng.*, 84, 253-304.
- [19] Alexandrov S., Kuo C.-Y., Jeng Y.-R. (2015) A Numerical Method for Determining the Strain Rate Intensity Factor Under Plane Strain Conditions, *Cont. Mech. Therm.*, 28, 977-992.
- [20] Hwang Y.-M., Huang T.-H., Alexandrov S. (2015) Manufacture of Gradient Microstructures of Magnesium Alloys Using Two - Stage Extrusion Dies, *Steel Res. Int.* 86, 956-961.
- [21] Alexandrov S., Jeng Y.-R., Hwang Y.-M. (2015) Generation of a Fine Grain Layer in the Vicinity of Frictional Interfaces in Direct Extrusion of AZ31 Alloy, *Trans ASME J. Manuf. Sci. Eng.* 137, Paper 051003.
- [22] Alexandrov S. (2009) The Strain Rate Intensity Factor and Its Applications: A Review, *Mater. Sci. Forum*, 623, 1-20.
- [23] Lyamina E., Nguyen T. (2016) Effect of the Yield Criterion on the Strain Rate and Plastic Work Rate Intensity Factors in Axisymmetric Flow, *Struct. Eng. Mech.* 58, 719-729.
- [24] Druyanov B., Nepershin R. *Problems of technological plasticity*. Amsterdam: Elsevier; 1994.
- [25] A. J. M. Spencer, "A theory of the failure of ductile materials reinforced by elastic fibres," *Int. J. Mech. Sci.*, vol. 7, pp. 197-209, 1965.
- [26] Hill, R., Lee, E.H., Tupper, S.J.: A method of numerical analysis of plastic flow in plane strain and its application to the compression of a ductile material between rough plates. *Trans. ASME J. Appl. Mech.* **18**, 46-52 (1951)
- [27] Hill, R.: *The Mathematical Theory of Plasticity*. Clarendon Press, Oxford (1950)